Characterization of Propagation Patterns with Omnipolar EGM in Epicardial Multi-Electrode Arrays

Jennifer Riccio[1], Alejandro Alcaine [1,2], Natasja M. S. de Groot[3], Richard Houben[4], Pablo Laguna[1,2], Juan Pablo Martinez[1,2]

1. BSICoS Group, Aragón Institute of Engineering Research (I3A), IIS Aragón, Universidad de Zaragoza, Zaragoza, Spain
2. CIBER in Bioengineering, Biomaterials and Nanomedicine (CIBER-BBN), Madrid, Spain
3. Translational Electrophysiology Unit, Department of Cardiology, Erasmus Medical Center, Rotterdam, The Netherlands
4. 2BMedical B.V., Maastricht, The Netherlands

MARIE CURIE ACTIONS

MY-ATRIA

1542 Universidad Zaragoza

ciber-bbn

BSICoS
Biomedical Signal Interpretation & Computational Simulation

Introduction

Clinical motivation

Atrial fibrillation (AF) is the most frequent cardiac arrhythmia

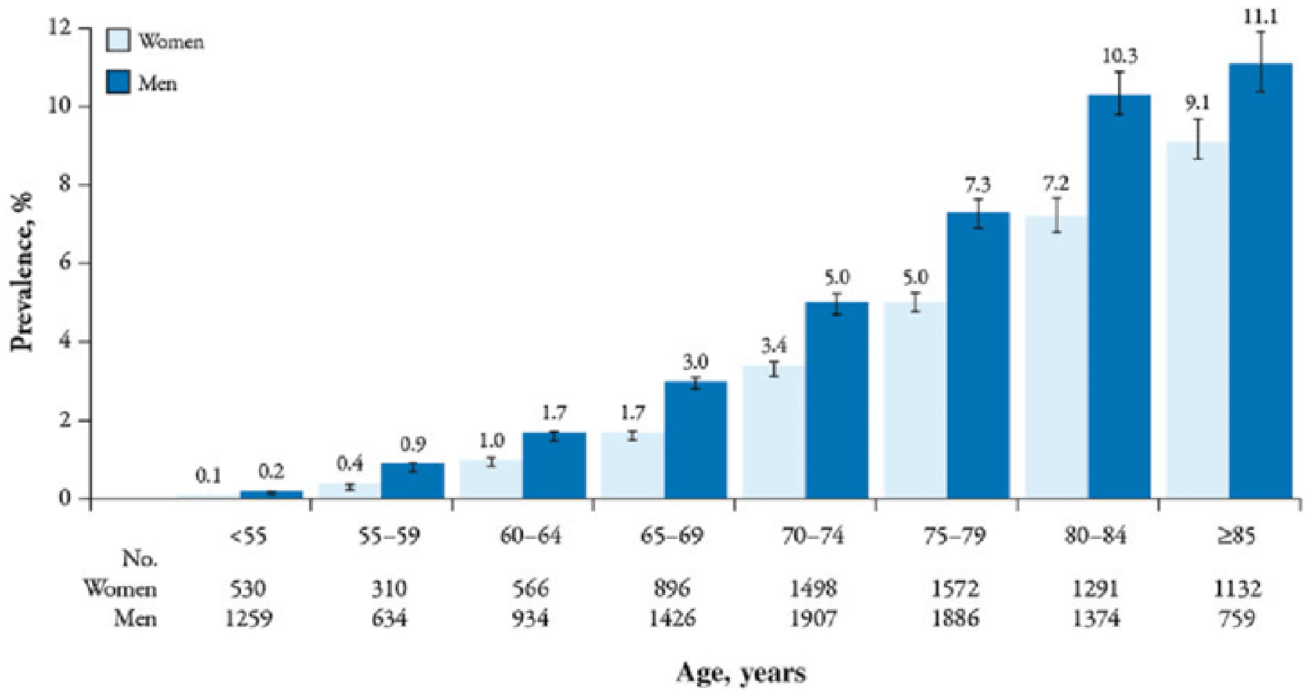

Ng et al., Cardiol Ther., 2013

Consequences of AF include heart failure, stroke, dementia, doubled mortality

Introduction

Why AF?

Incorrect interaction between activation mechanisms and an anomalous atrial substrate

- Multiple wavelet hypothesis
  Moe et al., Am Heart J., 1959

- Ectopic beats in pulmonary veins
  Haïsaguerre et al., N Engl J Med., 1998

- Rotor hypothesis
  Eckstein et al., Swiss Med Week., 2009

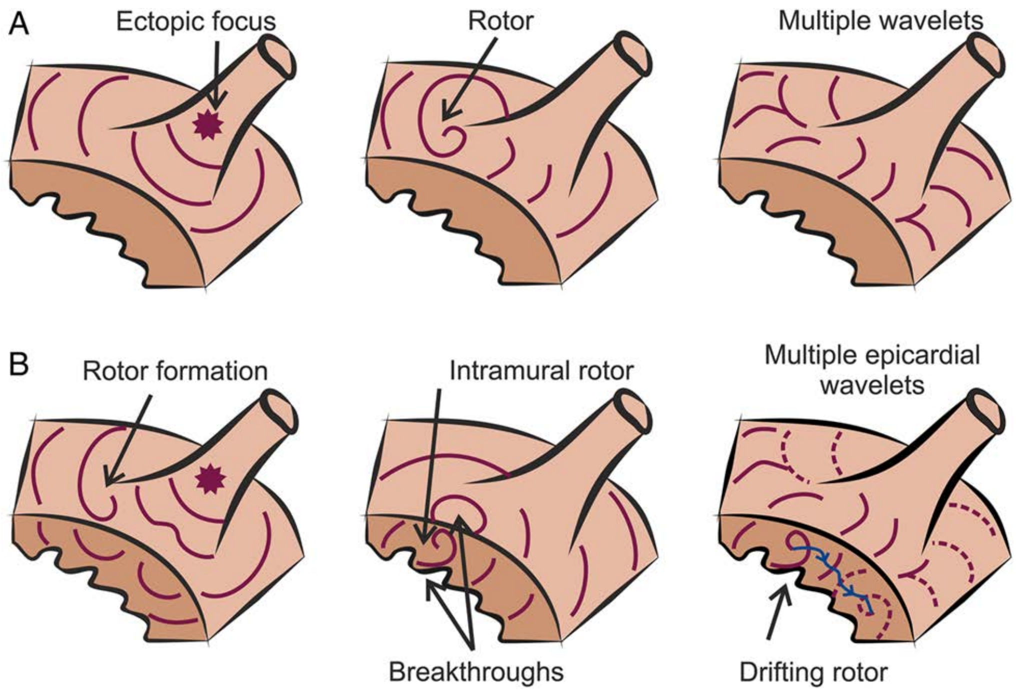

Guillem et al., CVR, 2016

BSICoS

Introduction

AF treatment: catheter ablation

Introduction of catheters to focally burn sites involved into the AF

↓

prevents ectopic impulses to trigger AF

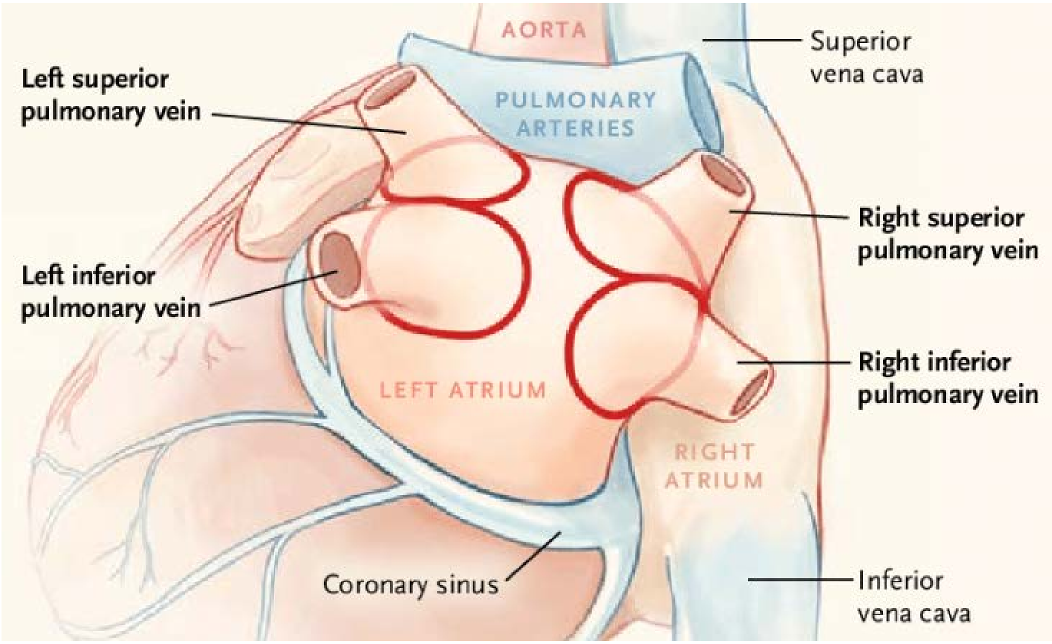

Verma et al., N Engl J Med., 2015

Introduction

Mechanisms of AF → characterization of atrial propagation using intracardiac electrograms (EGMs) ← **Catheter ablation**

Unipolar EGM (u-EGM)

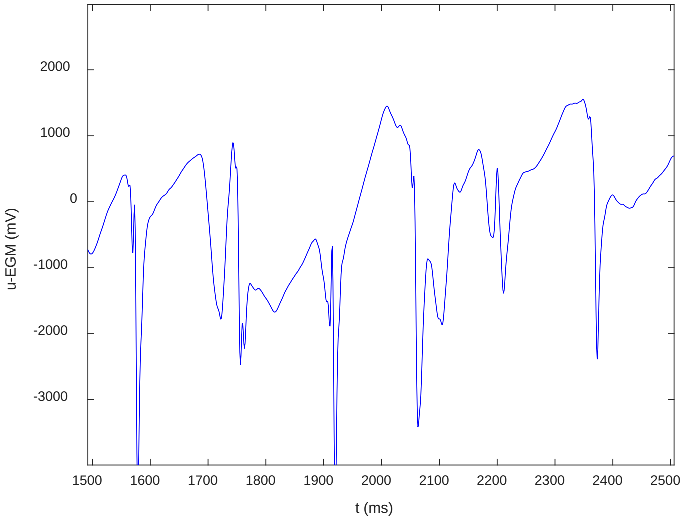

Omnipolar EGM (OP-EGM)

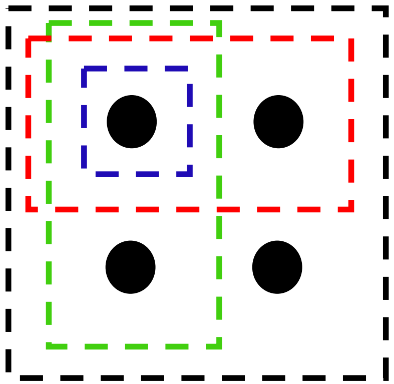

clique

Deno et al., IEEE TBME, 2017

Bipolar EGMs (b-EGMs)

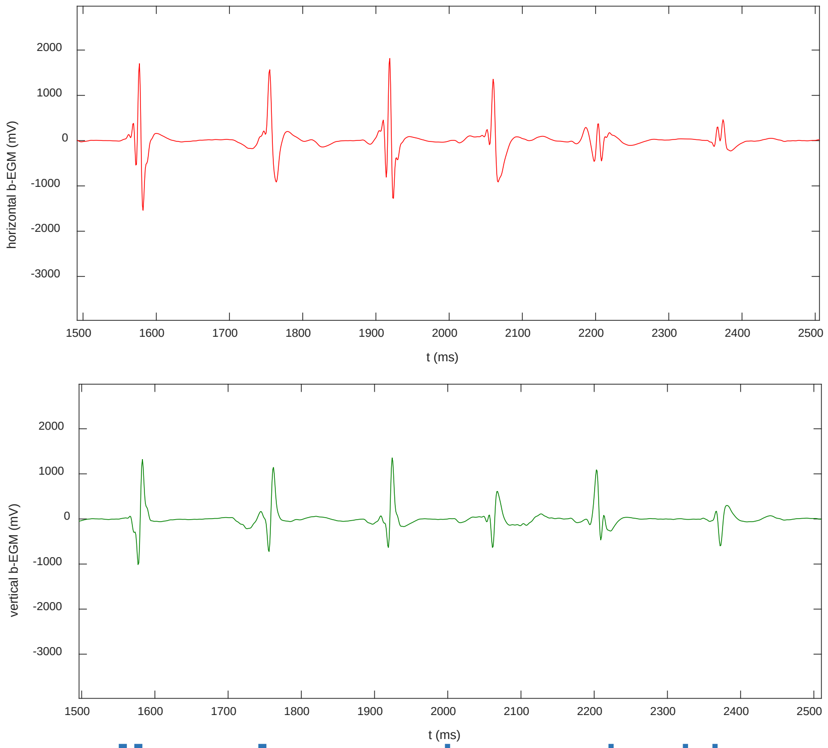

Aim

Accuracy evaluation of **conduction velocity** and **propagation direction** estimated with **OP-EGM method**

Materials

Simulated data

- 2-D slice
  (18 x 34 x 2 mm)

- Rectangular 8 x 16 multi-electrode array (MEA)
  (2 mm inter-electrode distance)

- Isotropic and anisotropic propagation patterns
  (anisotropy ratio = 0.5)

- Single activation focus at 3 locations

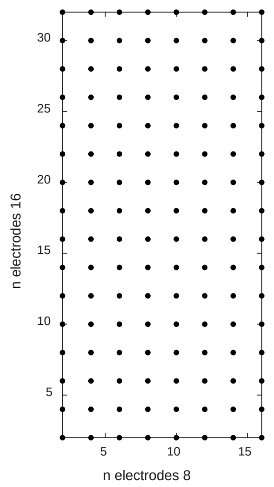

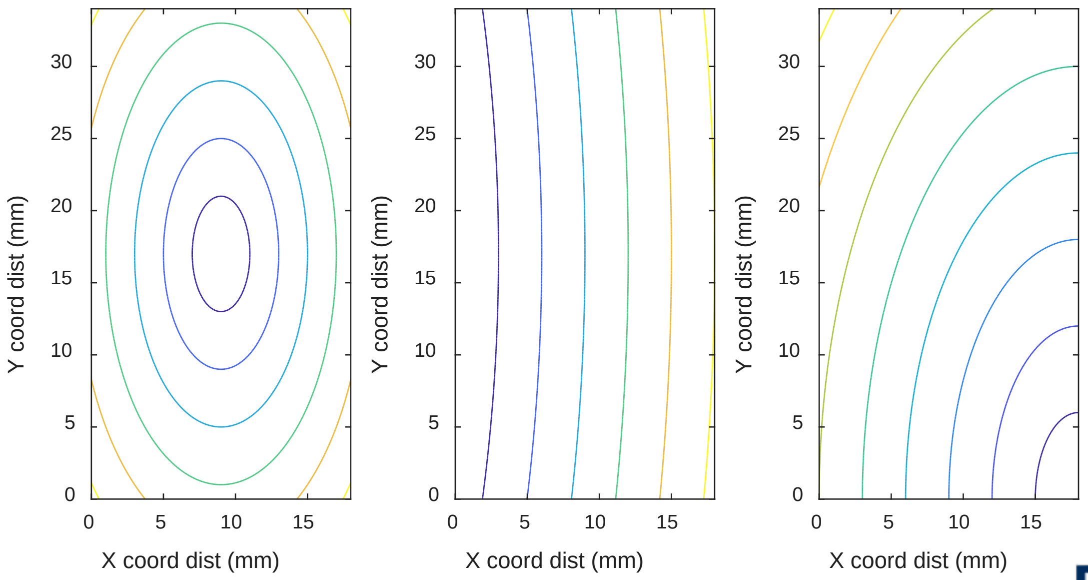

Materials

Clinical data

- Epicardial u-EGMs during sinus rhythm (SR) and (electrically induced) AF

- Rectangular 8 x 16 MEA
  (2 mm inter-electrode distance)

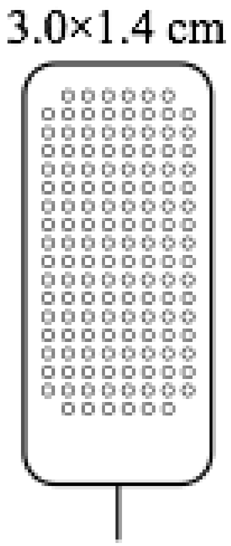

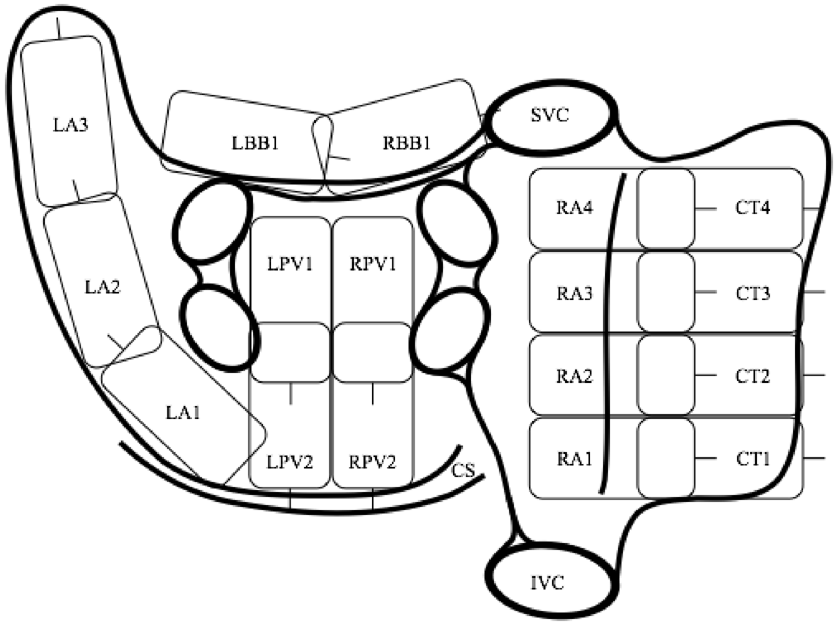

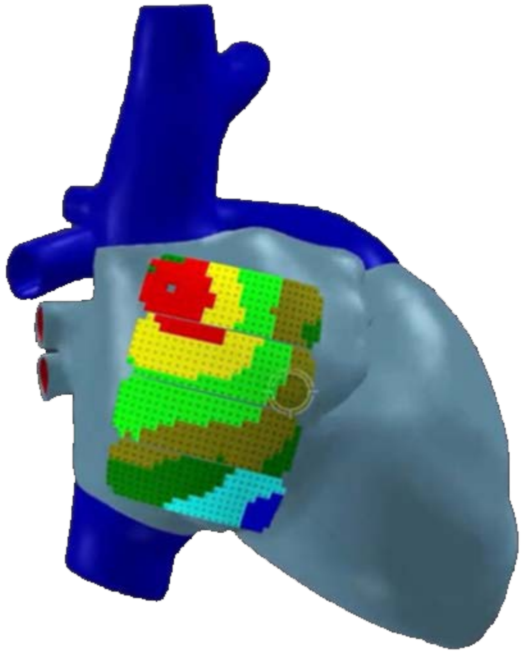

Yaksh et al., J Interv Card Electrophysiol., 2015

OP-EGM method

➢ **Locally homogeneous** and **plane** wave hypothesis

$$\boldsymbol{E}(t) = -\nabla\varphi(t)$$

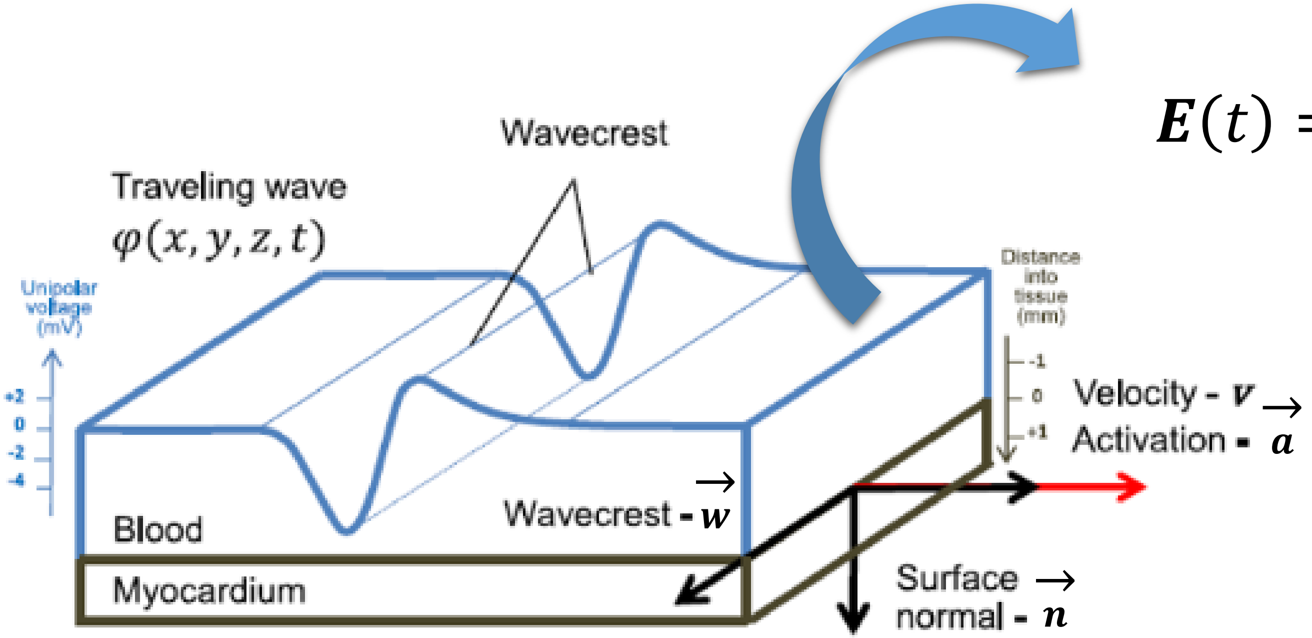

Deno et al., IEEE TBME, 2017

$$\boldsymbol{E}(t) = E_a(t)\,\vec{\boldsymbol{a}} + E_n(t)\,\vec{\boldsymbol{n}} + E_w(t)\,\vec{\boldsymbol{w}}$$

2-D

$$\boldsymbol{E_{2D}}(t) = E_a(t)\,\vec{\boldsymbol{a}} + E_w(t)\,\vec{\boldsymbol{w}}$$

Methods

OP-EGM method

$$\Delta_X = \begin{bmatrix} -\Delta & 0 & -\Delta & \Delta & 0 & -\Delta \\ 0 & \Delta & \Delta & \Delta & \Delta & 0 \end{bmatrix}$$

$$\boldsymbol{E}(t) = [E_x(t)\ E_y(t)]^T$$

$$\Delta_{\varphi}(t) = [\Delta\varphi_{12}(t)\ \Delta\varphi_{13}(t)\ \Delta\varphi_{14}(t)\ \Delta\varphi_{23}(t)\ \Delta\varphi_{24}(t)\ \Delta\varphi_{34}(t)]^T$$

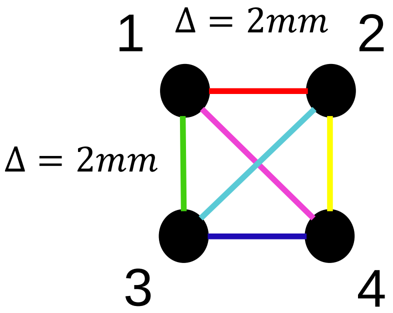

6 b-EGMs

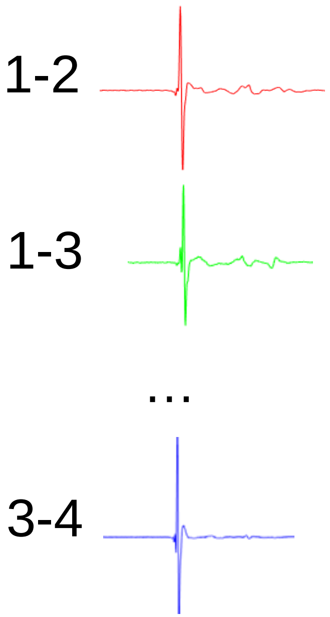

$$\Delta_{\varphi}(t) = -\Delta_X^T\, \boldsymbol{E}(t)$$

$$\boldsymbol{E}(t) = (-\Delta_X \Delta_X^T)^{-1} \Delta_X \Delta_{\varphi}(t) \qquad \text{LS}$$

Methods

OP-EGM method

$$\boldsymbol{E}(t)\cdot\boldsymbol{v}(t) = \dot{\varphi}(t) \quad \Rightarrow \quad \boldsymbol{v}(t) = \frac{\dot{\varphi}(t)}{E_a(t)}\vec{\boldsymbol{a}}$$

$$\vec{\boldsymbol{a}} = \max_{\vec{\boldsymbol{a}}} < \dot{\varphi}(t), \boldsymbol{E}(t)\cdot\vec{\boldsymbol{a}} >$$

$$\text{CV} = \|\boldsymbol{v}(t)\|$$

a:

$$\|\boldsymbol{v}(t)\| = \frac{[\dot{\varphi}(t)]_{pp}}{[E_a(t)]_{pp}}$$

b:

$$\|\boldsymbol{v}(t)\| = \frac{SD[\dot{\varphi}(t)]}{SD[E_a(t)]}$$

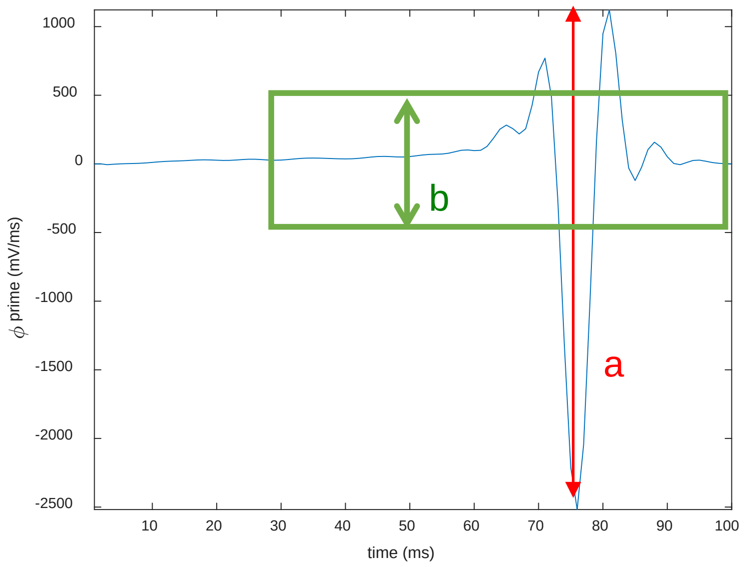

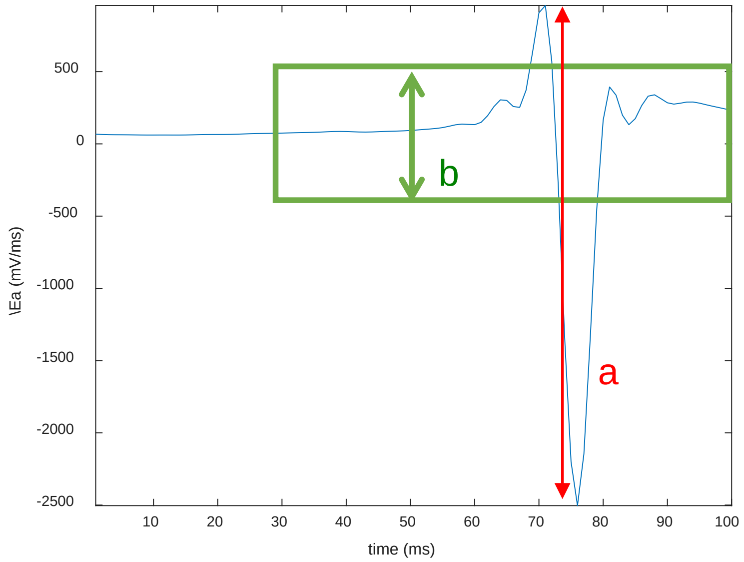

Methods

LATs-based estimation

- Linear propagation model in each clique: $t(x,y) = a_1 + a_2 x + a_3 y$

Bayly et al., IEEE TBME, 1998

$$v_x = \frac{\frac{\partial t}{\partial x}}{(\frac{\partial t}{\partial x})^2 + (\frac{\partial t}{\partial y})^2} = \frac{a_2}{a_2^2 + a_3^2}$$

$$v_y = \frac{\frac{\partial t}{\partial y}}{(\frac{\partial t}{\partial x})^2 + (\frac{\partial t}{\partial y})^2} = \frac{a_3}{a_2^2 + a_3^2}$$

Simulated data

Maximum negative slope of u-EGM

Clinical data

LATs manually detected

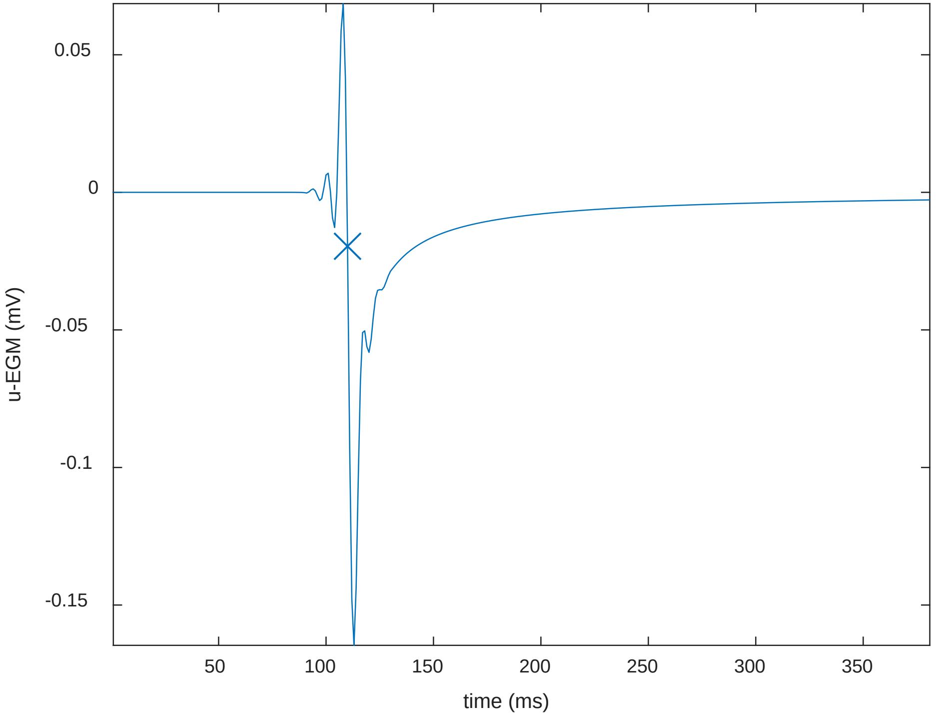

Methods

Conduction velocity maps and validation

Simulated data

Maps of CV and propagation directions

For each clique:

- True conduction velocity
- $\varepsilon_{CV} = CV^{estim} - CV^{true}$
- $\varepsilon_{\theta} = |\theta^{estim} - \theta^{true}|$

$\text{mean} \pm SD$ across the MEA

↓

mean total error

Clinical data

Maps of CV and propagation directions

Results and Discussion

Simulated data

Conduction velocity maps

$v_x = 0.6\ mm/ms \quad v_y = 1.2\ mm/ms$

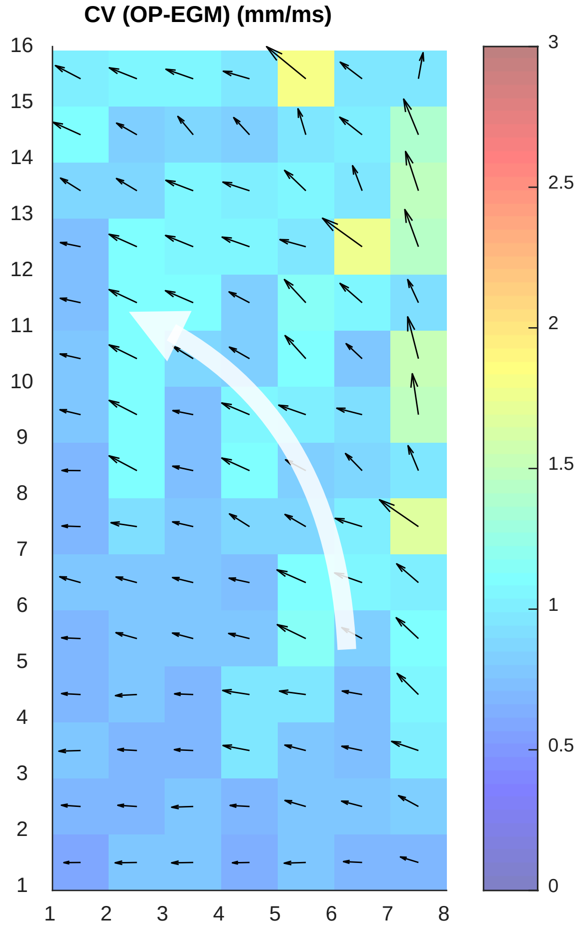

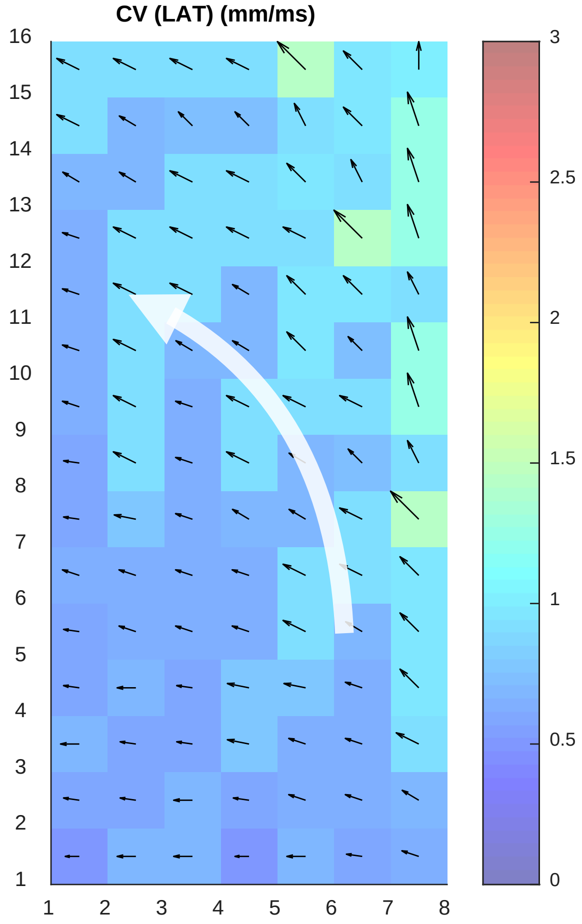

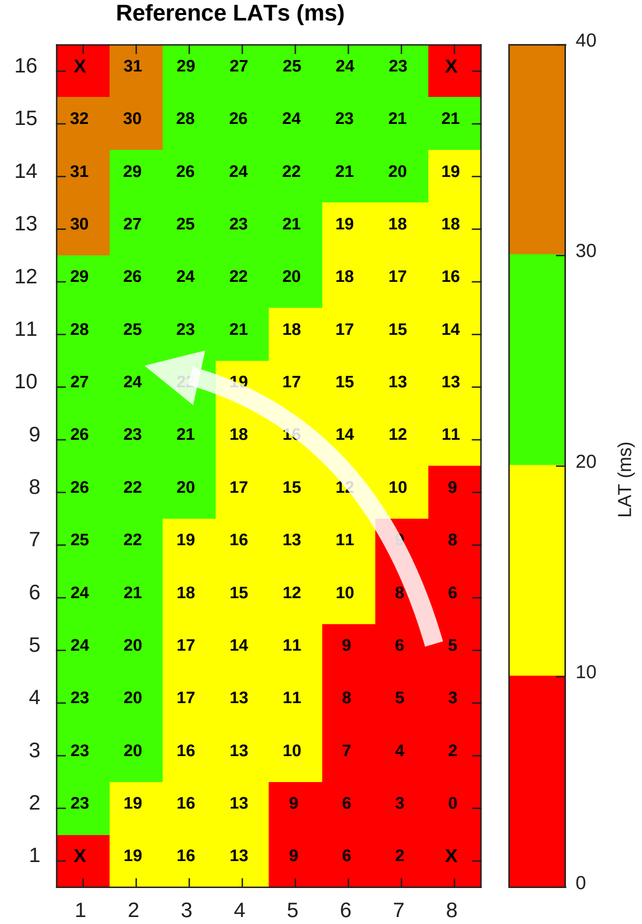

Results and Discussion

Validation

Simulated data

Simulated tissue characteristics	focus	ϵ_{CV}^{OP} (mm/ms)	ϵ_{CV}^{LAT} (mm/ms)	ϵ_{θ}^{OP} (deg)	ϵ_{θ}^{LAT} (deg)
Isotropic,	center	0.155 ± 0.067	0.015 ± 0.057	4.41 ± 3.9	2.35 ± 2.69
$v_x = v_y = 0.6$ mm/ms	bottom	0.121 ± 0.074	0.009 ± 0.062	3.78 ± 3.21	3.15 ± 2.86
	corner	0.177 ± 0.071	0.006 ± 0.057	7.28 ± 5.04	4.47 ± 3.27
Isotropic,	center	0.095 ± 0.322	0.045 ± 0.191	11.5 ± 11.8	6.99 ± 6.42
$v_x = v_y = 1$ mm/ms	bottom	0.053 ± 0.005	$0.003 \pm 2.11 \times 10^{-5}$	6.64 ± 4.3	4.35 ± 2.81
	corner	0.109 ± 0.257	0.016 ± 0.168	12 ± 8.42	7.56 ± 5.1
Anisotropic,	center	0.104 ± 0.173	0.013 ± 0.133	4.07 ± 3.32	3.95 ± 2.64
$v_x = 1.2$ mm/ms	bottom	0.117 ± 0.095	0.017 ± 0.075	1.43 ± 1.32	1.49 ± 2.35
$v_y = 0.6$ mm/ms	corner	0.118 ± 0.083	0.012 ± 0.071	6.47 ± 4.81	5.16 ± 3.5
Anisotropic,	center	0.143 ± 0.351	0.051 ± 0.222	6.3 ± 6.7	4.53 ± 3.61
$v_x = 0.6$ mm/ms	bottom	0.127 ± 0.067	0.012 ± 0.065	2.41 ± 1.95	3.04 ± 2.12
$v_y = 1.2$ mm/ms	corner	0.154 ± 0.174	0.017 ± 0.124	8.19 ± 6.82	5.16 ± 4.13
Anisotropic,	center	-0.049 ± 0.149	-0.019 ± 0.069	8.25 ± 6.13	5.67 ± 3.84
$v_x = 2$ mm/ms	bottom	0.056 ± 0.003	0.002 ± 7.710^{-4}	1.66 ± 0.974	1.09 ± 0.688
$v_y = 1$ mm/ms	corner	0.008 ± 0.187	-0.005 ± 0.11	11.8 ± 10.1	7.68 ± 6.59
Anisotropic,	center	-0.15 ± 0.253	-0.04 ± 0.141	11.7 ± 9	7.28 ± 52.7
$v_x = 1$ mm/ms	bottom	0.051 ± 0.008	$8.28 \times 10^{-4} \pm 0.004$	4.24 ± 2.52	2.75 ± 1.66
$v_y = 2$ mm/ms	corner	0.035 ± 0.382	0.027 ± 0.265	19.7 ± 21.3	10.3 ± 8.25
Mean total error		0.08 ± 0.205	0.007 ± 0.13	7.3 ± 8.96	4.86 ± 4.81

Results and Discussion

Clinical data

Conduction velocity maps

AF

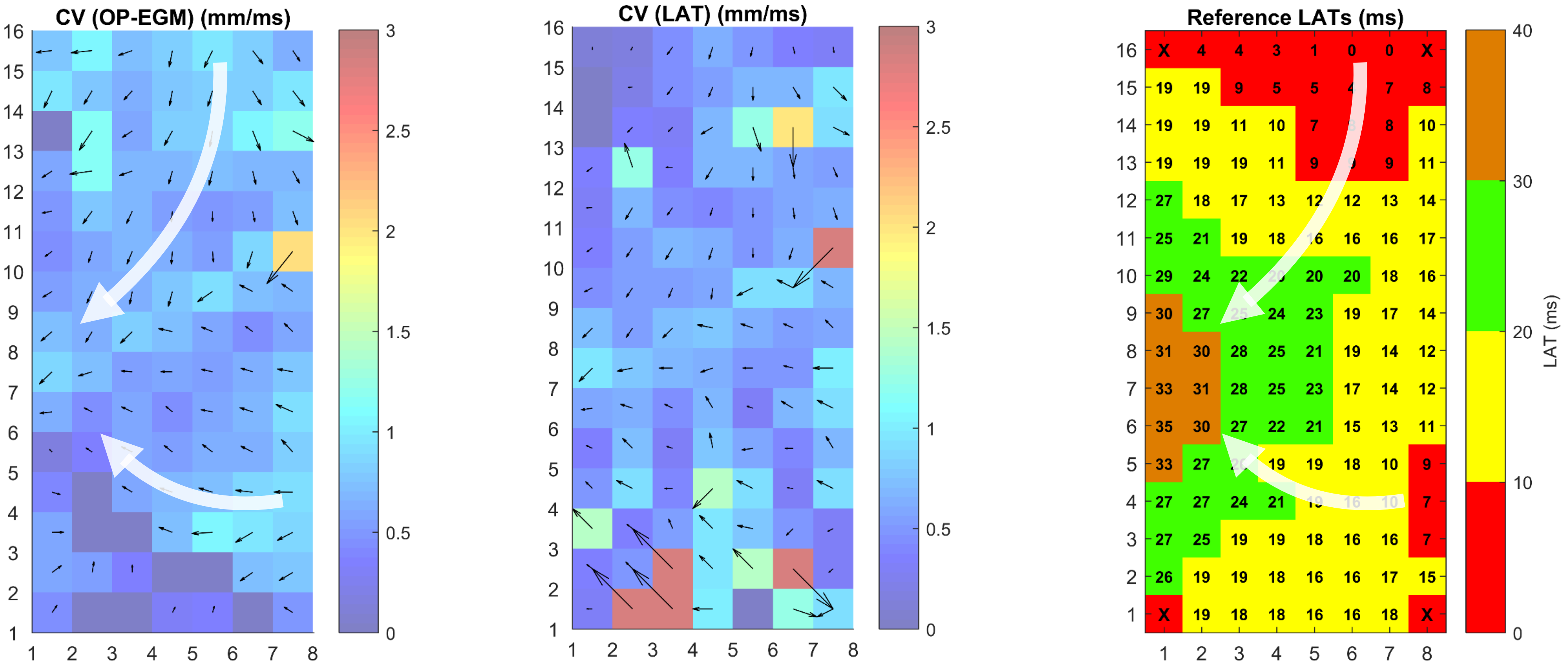

Results and Discussion

Clinical data

Conduction velocity maps

AF

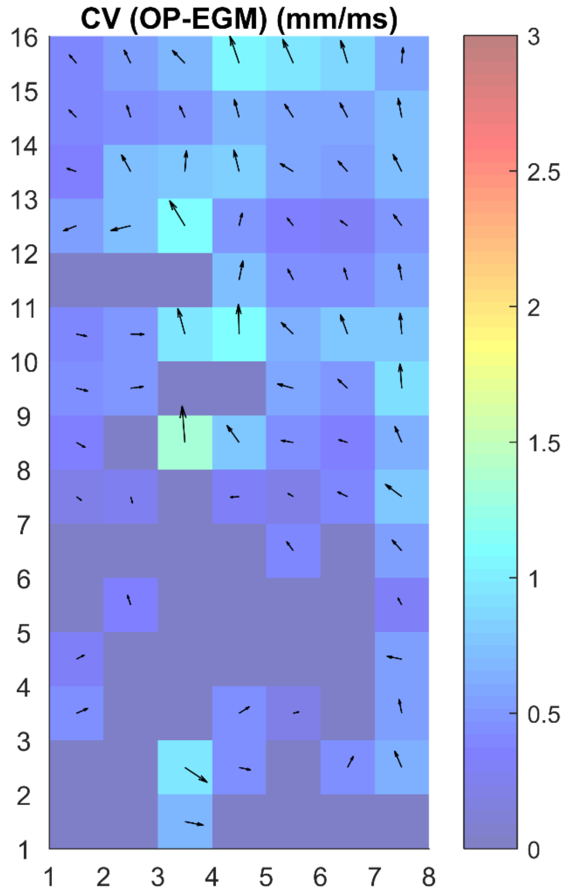

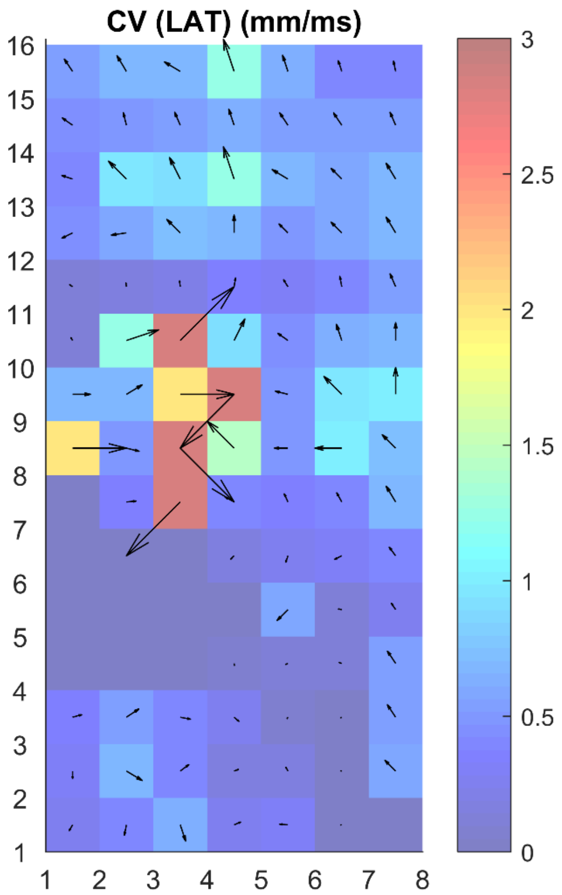

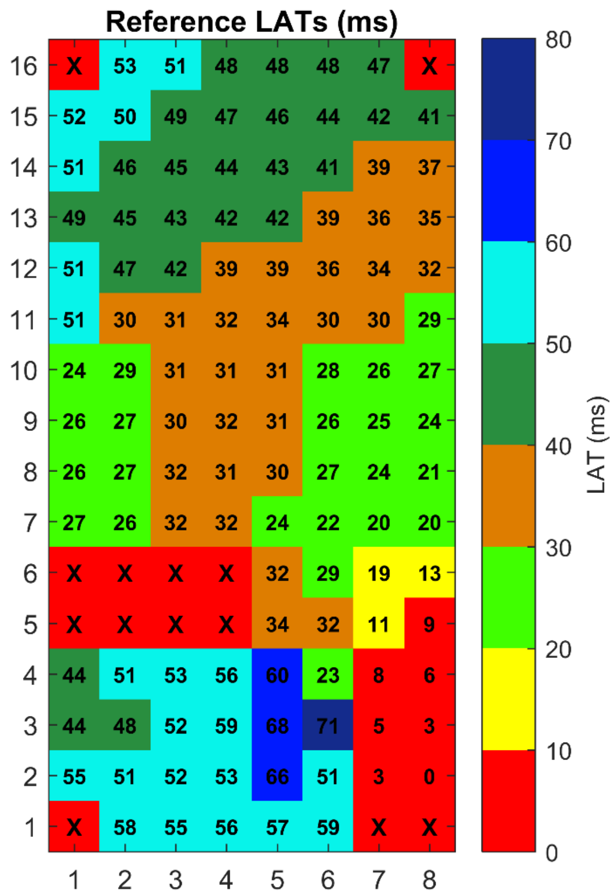

Conclusion

- Good concordance of OP-EGM and LAT-based estimations with the simulated propagation patterns

- Lower estimation errors provided by LATs-based approach in most of the cases

- Smoother and more coherent propagation patterns of OP-EGM method during AF

Conclusion

- OP-EGM does not require LAT detection
- OP-EGM exploits the spatio-temporal information encoded in the signal shape, avoiding the problems of b-EGMs
- OP-EGM assumes homogeneous and plane wave within each clique

Acknowledgments

This work is part of a project that has received funding from the European Union's Horizon 2020 research and innovation program under the Marie Skłodowska-Curie grant agreement No 766082.

It was also supported by projects DPI2016-75458-R (MINECO) and Aragon Government (Reference Group BSICoS T39-17R) cofunded by FEDER 2014-2020 “Building Europe from Aragon”.

Characterization of Propagation Patterns with Omnipolar EGM in Epicardial Multi-Electrode Arrays

Jennifer Riccio[1], Alejandro Alcaine [1,2],
Natasja M. S. de Groot[3], Richard Houben[4],
Pablo Laguna[1,2], Juan Pablo Martinez[1,2]

MARIE CURIE ACTIONS
MY-ATRIA
Universidad Zaragoza 1542
ciber-bbn
BSICoS
Biomedical Signal Interpretation & Computational Simulation